10.48047/jocaaa.2024.33.02.55
ISSN: 1521-1398
E-ISSN: 1572-9206

Magnetohydrodynamic Slip Flow of a Williamson Fluid Over a Melting Stretching Cylinder Chemical Reaction and Hall Current

Babu Lal Yadav[1], Anil Sharma[1], Manjeet Kumari[2]

[1]Department of Mathematics, University of Rajasthan, Jaipur, India
[2]LBS PG College, Jaipur
Email ID- math360degree1@gmail.com, anilsharma9414@gmail.com, manjeetyadav.muj@gmail.com-2024

Abstract: In present paper, we have investigated slip flow for MHD Williamson fluid flow over melting stretching surface cylinder through porous medium. Chemical reaction and Hall current effect is taken into consideration. Governing PDEs of the problem changed into nonlinear ODEs by using similarity transformation. Shooting technique with R-K Fourth order method is applied to find the solution of the problem. It illustrates and examines a detailed analysis of various parameters on velocity, temperature and concentration profiles are discussed and display graphically. The skin friction coefficient, local Nusselt number, local Sherwood number are tabulated. The present analysis results are compared with the available works in particular situations, and more agreement has been observed.

Keyword: Melting surface, Williamson fluid, chemical reaction, slip flow, Hall current, ion-slip.

Introduction:

Non-Newtonian fluids are generally classified according to their properties into categories such as visco-inelastic, visco-elastic, polar, anisotropic, and micro structured fluids. Among these, the Williamson model represents an important type of visco-inelastic fluid. Several studies have explored its behavior under different physical conditions. For instance, Alam et al. [1] investigated boundary-layer flows of Williamson fluids, while Williamson [2] originally introduced the theoretical model. Dapra et al. [3] provided perturbation solutions for Williamson fluid motion, and Gorla et al. [4] examined convective heat transfer in Williamson nanofluids. Additionally, Khan et al. [5] discussed chemically reactive boundary-layer flow of this fluid, and Monica et al. [6] analyzed the influence of thermal radiation on Williamson fluid flow over a nonlinearly stretching surface. Gorla et al. [7] examined chemical reactive slip flow for Williamson nano-fluid with nonlinear thermal radiation over a stretching sheet. Nadeem et al. [8-11] investigated the various physical parameter effects on Williamson fluid flow and heat transfer. Humane PP et al. [12] examined that MHD Casson-Williamson double-diffusive nanofluid flow past an inclined magnetic stretching sheet

Magnetohydrodynamics (MHD) focuses on the behavior of electrically conducting fluids in the presence of magnetic fields. Examples of such fluids include plasma, liquid metals, and even

10.48047/jocaaa.2024.33.02.55
ISSN: 1521-1398
E-ISSN: 1572-9206

saline water. MHD has diverse applications in areas like astrophysics, engineering systems, sensor technology, and targeted drug delivery using magnetic fields. In astrophysical phenomena, magnetic forces are especially significant as they influence the formation of stars. Because of these wide-ranging applications and fundamental importance, MHD flows continue to attract considerable attention from researchers worldwide. Humane PP et al. [13 studied that Chemical reaction and thermal radiation effects on magnetohydrodynamics flow of Casson–Williamson nanofluid. Roy, N. C. [14] studied that Williamson Fluid Flow Having Microorganisms Over a Permeable Shrinking Sheet. Variable fluid property for MHD viscous fluid containing Gyrotactic Microorganisms flow over a permeable stretching sheet investigated by Manjeet et al. [15]. Several researchers (Nadeem et al. [16], Shalini Jain et al. [17], Malik et al. [18], Darji et al. [19], Narayana et al. [20]) investigated the MHD effect on various types of Newtonian and non-Newtonian fluid.

Heat transfer processes involving melting in non-Newtonian fluids are of great significance in thermal engineering, with applications ranging from permafrost thawing and petroleum recovery to magma solidification and thermal insulation. Consequently, extensive experimental and theoretical research has been carried out to understand the kinetics of heat transfer when it is influenced by melting and solidification phenomena. The process of melting of ice placed in a hot stream of air at a steady state was first reported by Roberts [21]. Several researchers (Tien et al. [22], Epstein et al. [23], Gorla et al. [24], Manjeet Kumari et al. [25] and Gorla et al. [26]) examined melting heating transfer in non-Newtonian fluid.

The present analysis considers slip-flow heat and mass transfer of a magnetohydrodynamic (MHD) Williamson fluid over a stretching cylindrical surface undergoing melting within a porous medium. Owing to the importance of heat transfer in diverse industrial, commercial, and engineering systems, particular attention is directed towards understanding the thermal features of this configuration. The mathematical formulation incorporates the influence of chemical reactions together with Hall current effects. Numerical solutions are obtained using the fourth-order Runge–Kutta approach, and the corresponding results are demonstrated both graphically and through numerical tables.

Problem statement and mathematical formulation-:

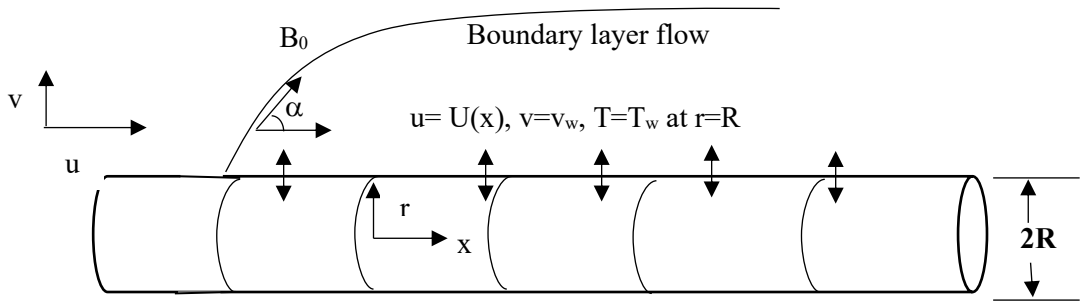

10.48047/jocaaa.2024.33.02.55
ISSN: 1521-1398

Figure 1. Schematic diagram of boundary layer flow over permeable cylinder

A steady incompressible non-Newtonian boundary-layer flow is analyzed over a stretching cylindrical surface undergoing melting, as depicted in Fig. 1. The cylinder is oriented along the x-axis, with the radial direction represented by r. A transverse magnetic field is imposed in the radial direction, and the effect of the induced magnetic field is also taken. The cylinder is placed within a porous medium, and both the fluid and the porous structure are assumed to be in local thermal equilibrium. The surface of the stretching cylinder is maintained at a fixed temperature T_w , while the ambient fluid temperature is T∞. Under these assumptions, the continuity, momentum, and energy equations governing the problem are formulated as follows:

$$\frac{\partial(rv)}{\partial r}+\frac{\partial(ru)}{\partial x}=0 \tag{1}$$

$$u\frac{\partial u}{\partial x}+v\frac{\partial u}{\partial r}=\upsilon\left[\frac{1}{r}\frac{\partial u}{\partial r}+\frac{\partial^2 u}{\partial r^2}+\frac{\Gamma}{\sqrt{2}r}\left(\frac{\partial u}{\partial r}\right)^2+\sqrt{2}\Gamma\frac{\partial u}{\partial r}\frac{\partial^2 u}{\partial r^2}\right]-\frac{1}{\rho}\frac{\sigma B_0{}^2(\alpha_e u)}{\alpha_e{}^2+\beta_e{}^2}-\frac{\upsilon\phi_p}{kp}u \tag{2}$$

$$u\frac{\partial T}{\partial x}+v\frac{\partial T}{\partial r}=\frac{1}{r}\frac{\partial}{\partial r}\left(\alpha r\frac{\partial T}{\partial r}\right)-\frac{\sigma B_0{}^2\ u^2}{\alpha_e{}^2+\beta_e{}^2}\frac{1}{\rho c_p}-\frac{1}{\rho c_p}\frac{\partial q_r}{\partial r} \tag{3}$$

$$u\frac{\partial C}{\partial x}+v\frac{\partial C}{\partial r}=D_B\left(\frac{\partial^2 C}{\partial r^2}+\frac{1}{r}\frac{\partial C}{\partial r}\right)-kn(\mathrm{C}-\mathrm{C}_\infty) \tag{4}$$

Boundary condition are following such as

$$u=u_w,\ \ v=\frac{k}{\rho\left(\beta+c_s(\mathrm{T}_w-\mathrm{T}_0)\right)}\frac{\partial T}{\partial r},\ T=T_w, C=C_w \quad at\ \ r=R$$

$$u\to 0, \qquad T=T_\infty, \qquad C=C\infty \quad at\ \ r=R \tag{5}$$

The stretching velocity $U(x)=\frac{U_0 x}{l}$ and the U_0 is the reference velocity l, T_∞ and T_W are the characteristic length, extrema temperature and the wall temperature. On expanding T^4, in a Taylor series about T_∞ , on neglecting higher order term, we get

$$T^4\approx T_\infty{}^4+4T_\infty{}^3T$$

$$\frac{\partial q_r}{\partial r}=\frac{\partial}{\partial r}\left(\frac{-4\sigma^*}{3k}\frac{\partial T^4}{\partial r}\right)=\frac{\partial}{\partial r}\left(\frac{-4\sigma^*}{3k}\frac{\partial(T_\infty{}^4+4T_\infty{}^3T-4T_\infty{}^3T_\infty)}{\partial r}\right)=\frac{-16\sigma^*T_\infty{}^3}{3k}\frac{\partial^2 T}{\partial r^2}$$

10.48047/jocaaa.2024.33.02.55
ISSN: 1521-1398
E-ISSN: 1572-9206

The stream function is introducing $u=\frac{1}{r}\frac{\partial\psi}{\partial r}$, $v=-\frac{1}{r}\frac{\partial\psi}{\partial x}$ and the similarly transformation for the following momentum and temperature equation are defined as

$$\eta=\frac{r^2-R^2}{2R}\sqrt{\frac{U}{\nu x}},\ \psi=\sqrt{U\nu x}R\,f(\eta),\ \theta=\frac{T-T_W}{T_W-T_\infty}\text{ and }\alpha=\alpha_\infty\left(1+\varepsilon\theta\right) \tag{6}$$

Where α_∞ is the thermal conductivity at a large distance away from the cylinder and ε is the small amount of thermal conductivity.

The equation (2) to (3) using the equation (5) to make a non-dimension form such as

$$f'''\left((1+2\eta\gamma)+We(1+2\eta\gamma)^{3/2}f''\right)-f'^2+ff''+2\gamma f''+\frac{3}{2}\gamma We(1+2\eta\gamma)^{1/2}f''^2 -\frac{\alpha_e Mf'}{\alpha_e^{\,2}+\beta_e^{\,2}}-Kpf'=0 \tag{7}$$

$$\theta''(1+2\eta\gamma)\left(1+\varepsilon\theta+\frac{4R}{3}\right)+\Pr f\theta'+2\theta'\gamma(1+\varepsilon\theta+\frac{2}{3}R)+(1+2\eta\gamma)\varepsilon\theta'^2+\frac{M\Pr Ecf'^2}{\alpha_e^{\,2}+\beta_e^{\,2}}=0 \tag{8}$$

$$\phi''(1+2\eta\gamma)+2\phi'\gamma-Sc\left(Kn\phi-f\phi'\right)=0 \tag{9}$$

Boundary condition is given below

$$\begin{aligned}&\Pr f+Me\theta'=0,\ f'=1,\ \theta=1,\ \phi=1\quad at\quad \eta=0\\ &f'\to 0,\ \theta\to 0,\ \phi\to 0\qquad at\quad \eta\to\infty\end{aligned} \tag{10}$$

The dimensionless number $\Pr$, γ, M, R, Kp and We are the Prandtl number, curvature parameter, magnetic parameter, radiation parameter, permeability parameter and Williamson fluid parameter, defined as

$$\gamma=\frac{1}{R}\sqrt{\frac{x\nu}{U}},\ \Pr=\frac{\nu}{\alpha_\infty},M=\frac{\sigma lB_0^{\,2}}{U_0\rho},Kp=\frac{\nu l}{k^*U_0},R=\frac{4\sigma^*T_\infty^{\,3}}{3k_1\alpha_\infty\rho c_p}\ We=\Gamma\sqrt{\frac{2U^3}{\nu x}}$$

Where, $\sigma=(e^2n_et_e)/m_e$: electrical conductivity; $\alpha=1+\beta_e\beta_i$, here $\beta_e=\omega_e t_e$: the hall parameter; $\beta_i=en_eB_0/((1+n_e/n_a)k_{ai})$:the ion-slip parameter; $\omega_e=eB_0/m_e$: the electron frequency; e: the electron charge; n_e: the electron number density, t_e: the electron collision time; m_e: the mass of the electron; c_p: specific heat at constant pressure of the fluid; n_a is the neutral particle number density, k_{ai} is the friction coefficient between ions and neutral particles.

In this analysis, the key engineering parameters are the skin-friction coefficient, the local Nusselt number, and the local Sherwood number. Their respective mathematical representations are

10.48047/jocaaa.2024.33.02.55
ISSN: 1521-1398
E-ISSN: 1572-9206

given by: $C_f = \frac{\tau_w}{\rho U_w^2}$, $Nu_x = \frac{-xq_w}{(T_w - T_\infty)} \frac{\partial T}{\partial r}\Big|_{r=0}$ and $Sh_x = \frac{x J_w}{D_B(C_w - C_\infty)}$

(11) where $\tau_w = \mu \left[\frac{\partial u}{\partial r} + \frac{\Gamma}{2}\left(\frac{\partial u}{\partial r}\right)^2 \right]\Big|_{y=0}$

$$q_w = -\left(k + \frac{16\sigma T_\infty^3}{3k^*} \right)\left(\frac{\partial T}{\partial r}\right)\Big|_{r=0} \text{ ; surface heat flux}$$

$$J_w = -D_B \left(\frac{\partial C}{\partial r}\right)_{r=0} \text{ ; surface mass flux} \quad (12)$$

On substituting value from equation (12) in to equation (11), we get the following dimensionless expressions for skin friction coefficient, local Nusselt number and local Sherwood number as given below:

$$C_f \, \mathrm{Re}_x^{\frac{1}{2}} = \left(f'' + \frac{We}{2} f''^2 \right)\Big|_{\eta=0} \quad (13)$$

$$Nu \, \mathrm{Re}_x^{\frac{-1}{2}} = -\left(1 + \frac{4R}{3}\right)\theta'(0), \quad (14)$$

$$Sh \, \mathrm{Re}^{-1/2} = -\phi'(0) \quad (15)$$

Table-1

Comparison of $-f''(0)$ for different values M in the absence of the parameters Me= M=Kp= $\beta_1 = \beta_e = \varepsilon = \gamma$ =R=0.0, Pr= 0.72					
M	Anderson et al. [27]	Prasad et al. [28]	Mukhopadhyay et al. [29]	Palani et al [30]	Present study
0.0	1.000000	1.000174	1.000173	1.000000	1.000008388
0.5	1.224900	1.224753	1.224753	1.224745	1.224744963
1	1.414000	1.414449	1.414450	1.414214	1.414213545
1.5	1.581000	1.581139	1.581140	1.581139	1.581138868
2	1.732000	1.732203	1.732203	1.732051	1.732050878

10.48047/jocaaa.2024.33.02.55
ISSN: 1521-1398
E-ISSN: 1572-9206

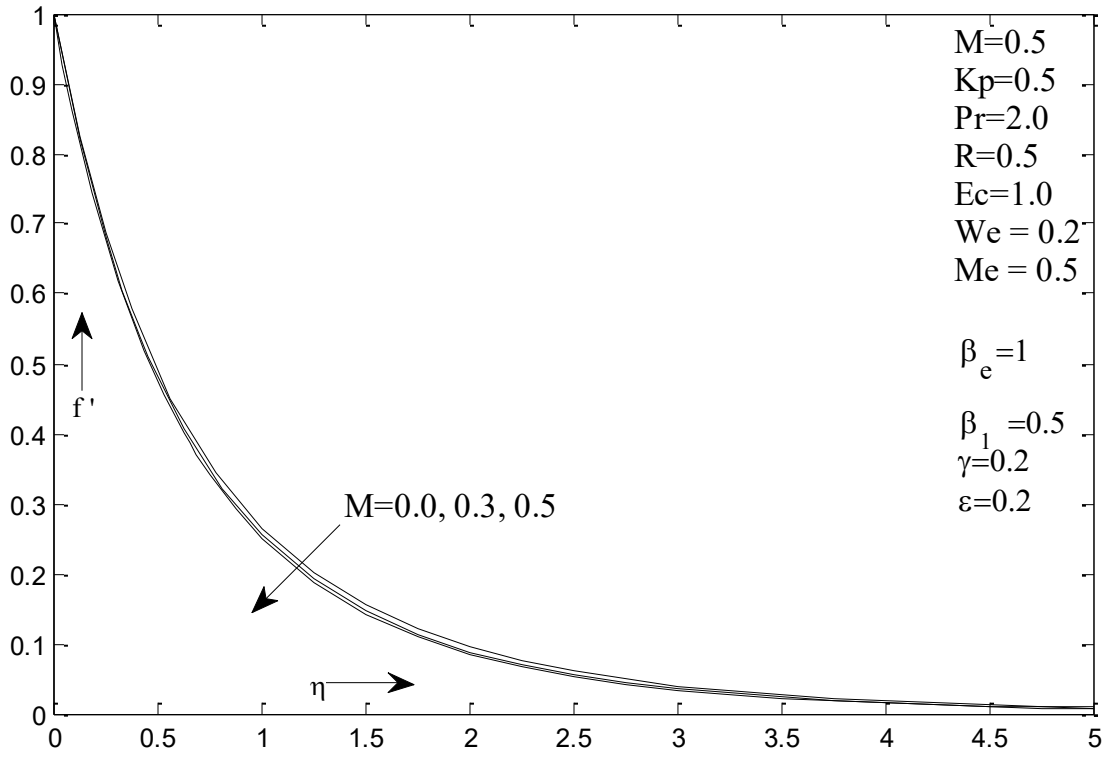

Figure 2 Influence of M on Momentum profile

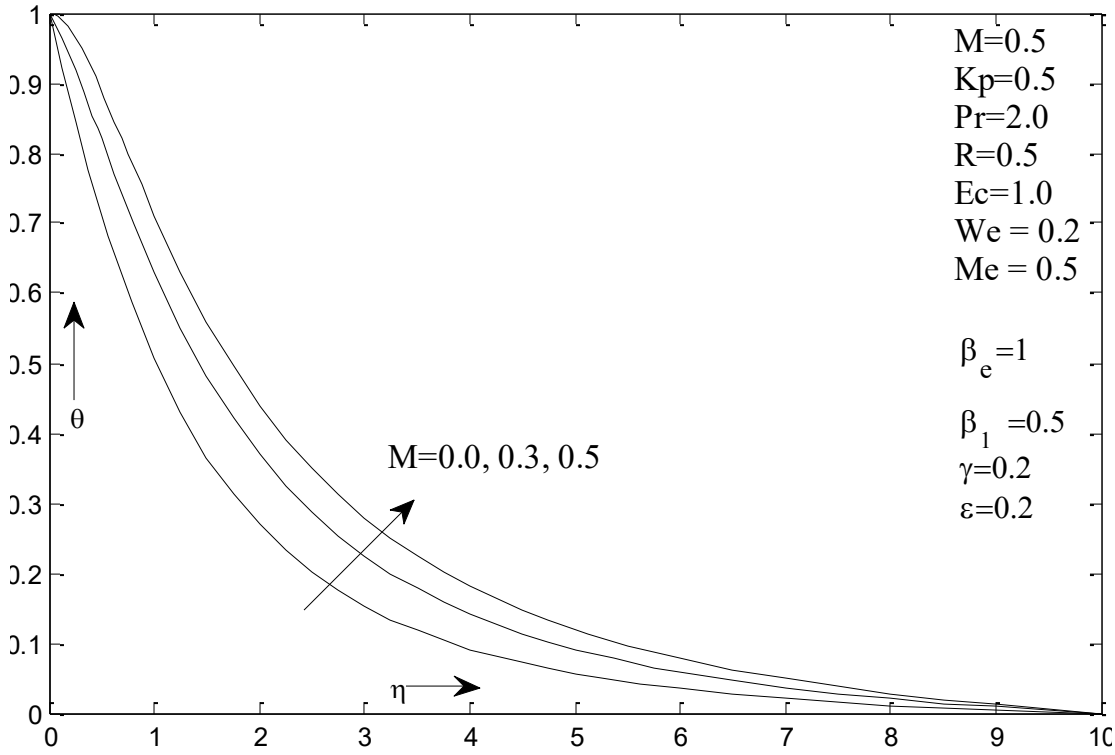

10.48047/jocaaa.2024.33.02.55
ISSN: 1521-1398
E-ISSN: 1572-9206

Figure 3 Influence of M on Temperature profile

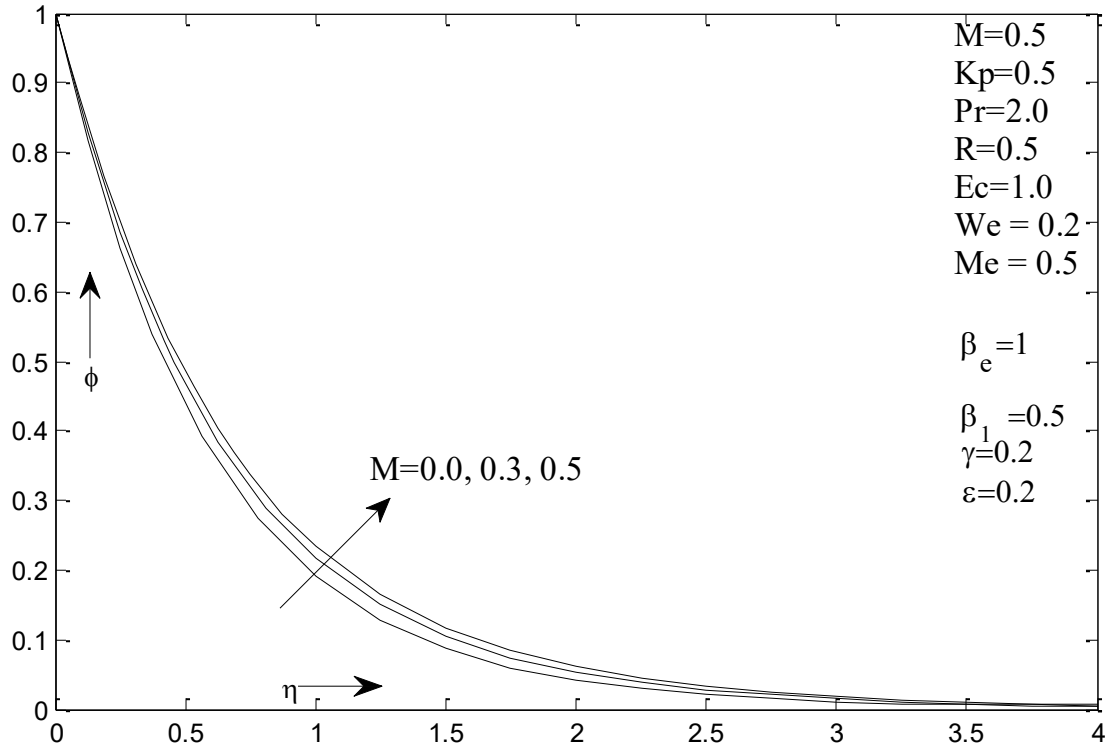

Figure 4 Influence of M on mass profile

10.48047/jocaaa.2024.33.02.55
ISSN: 1521-1398
E-ISSN: 1572-9206

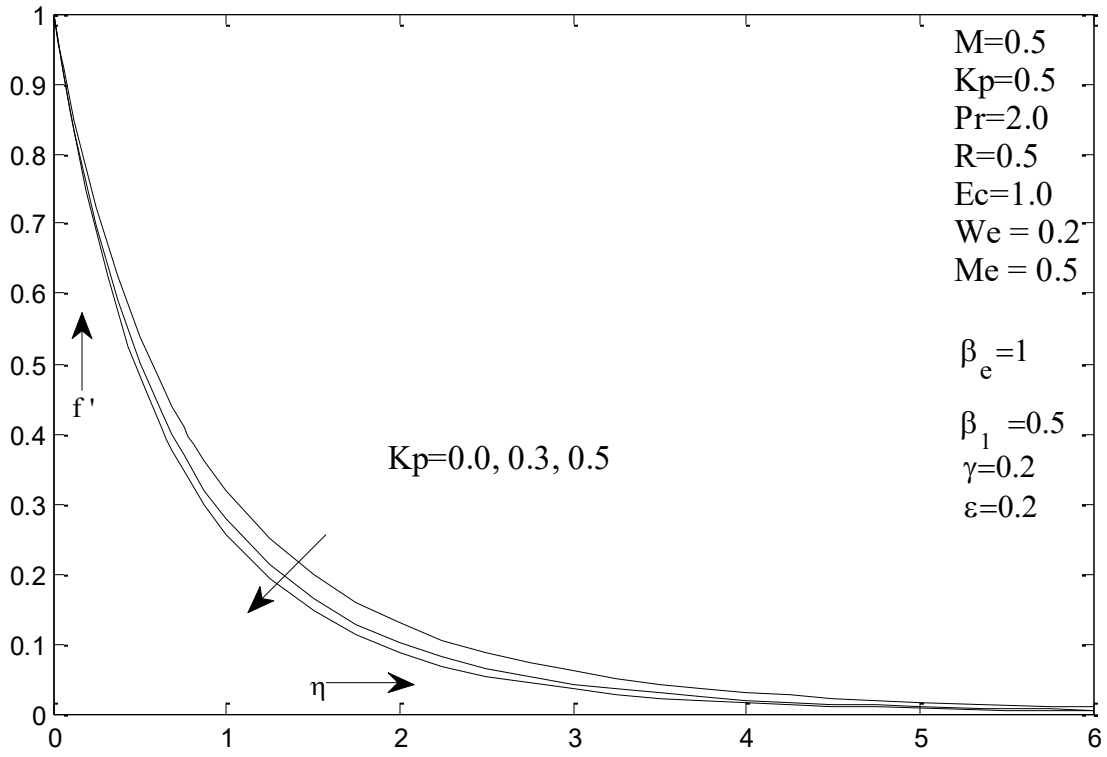

Figure 5 Influence of Kp on Momentum profile

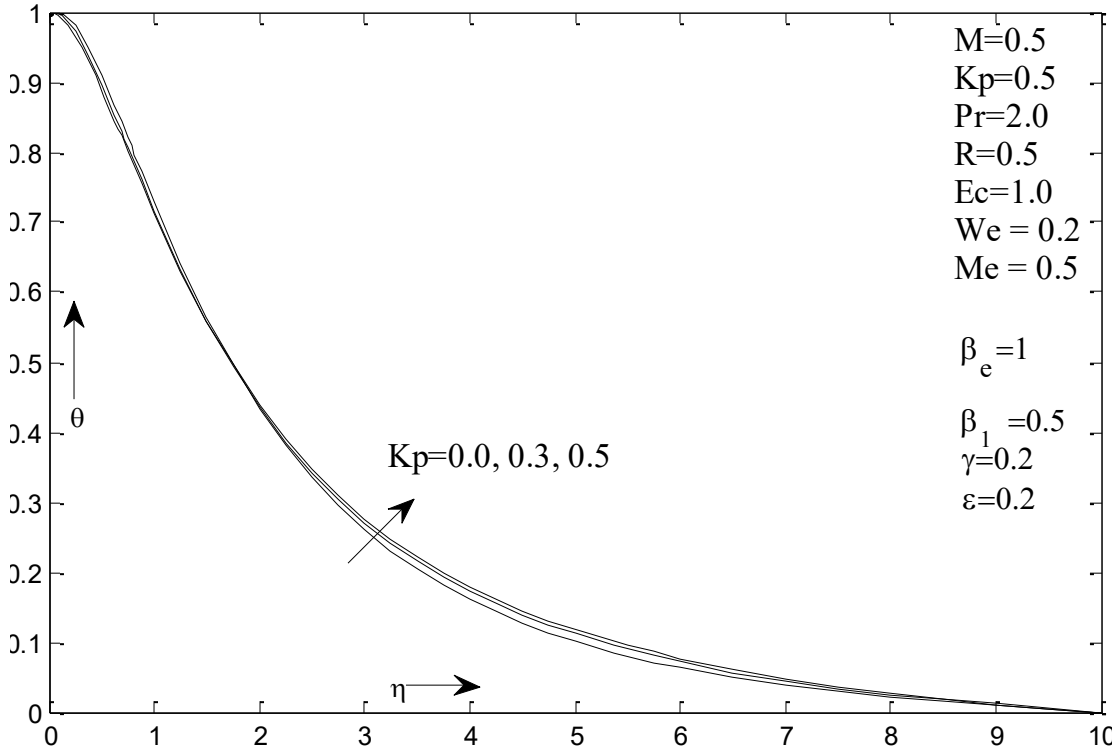

10.48047/jocaaa.2024.33.02.55
ISSN: 1521-1398
E-ISSN: 1572-9206

Figure 6 Influence of Kp on Temperature profile

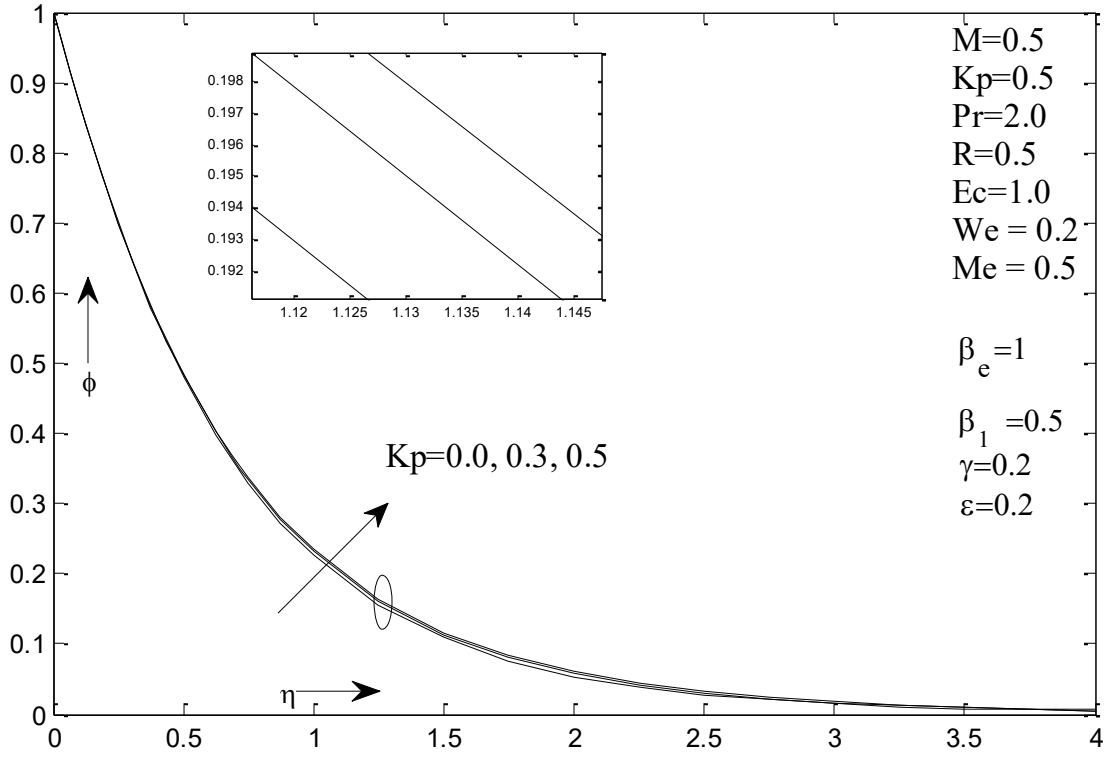

Figure 7 Influence of Kp on mass profile

10.48047/jocaaa.2024.33.02.55
ISSN: 1521-1398
E-ISSN: 1572-9206

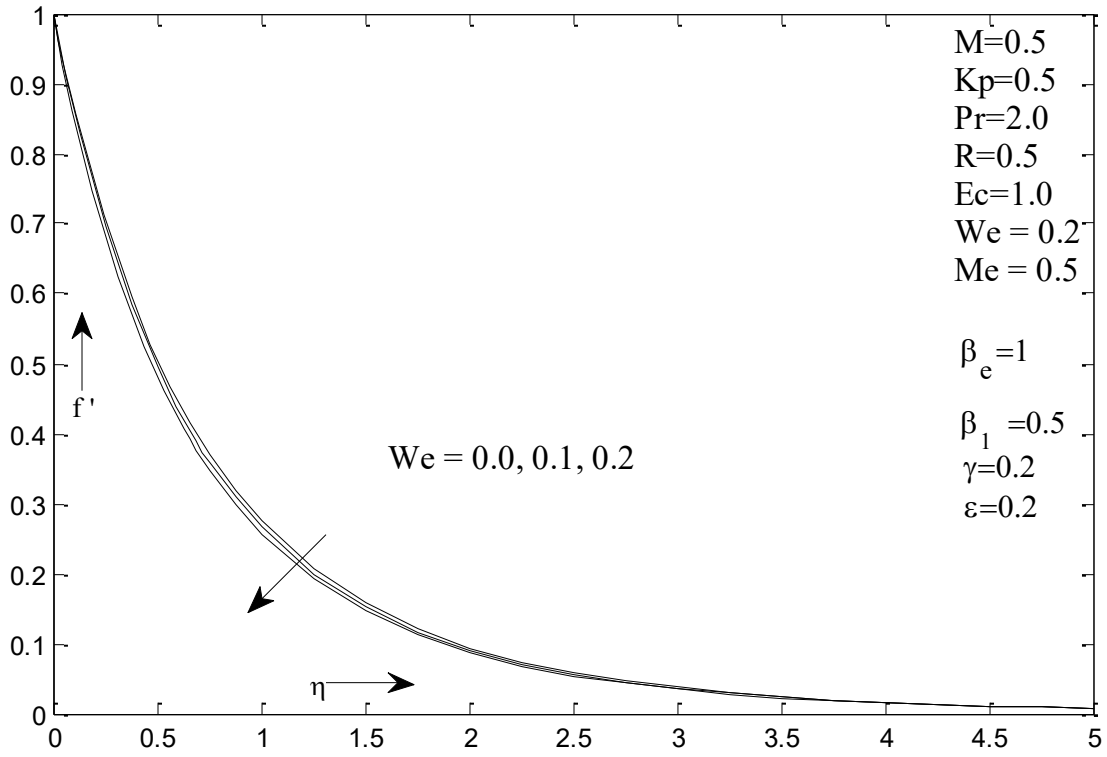

Figure 8 Influence of We on Momentum profile

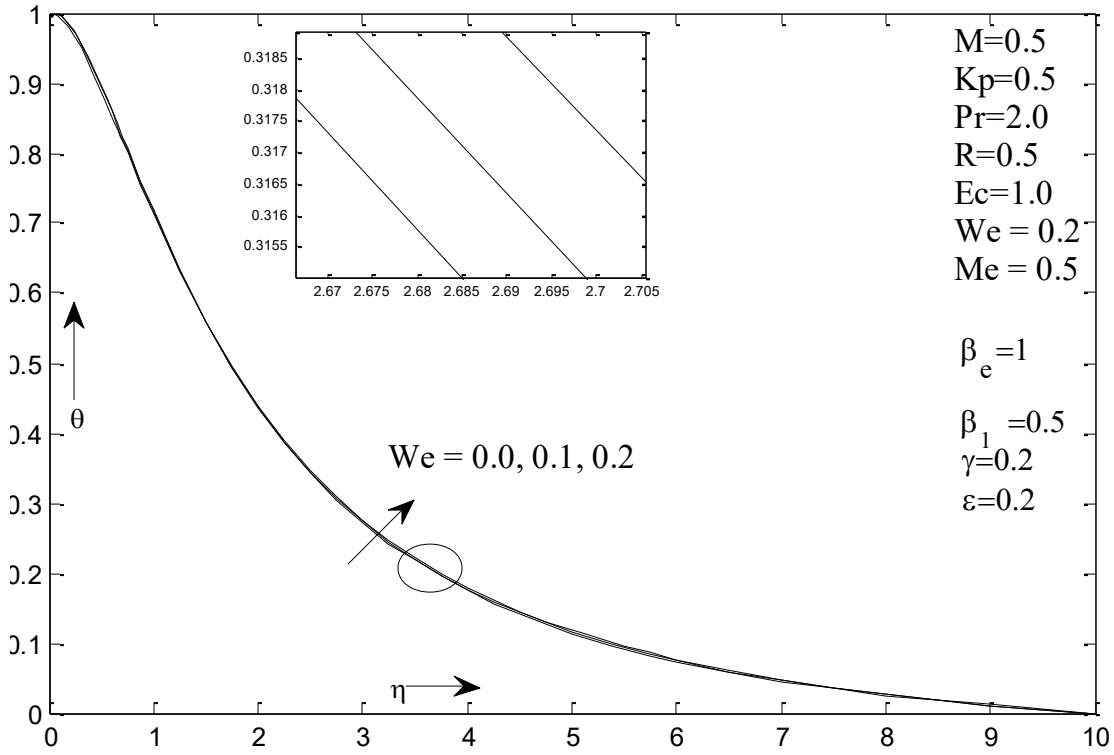

10.48047/jocaaa.2024.33.02.55
ISSN: 1521-1398
E-ISSN: 1572-9206

Figure 9 Influence of We on Temperature profile

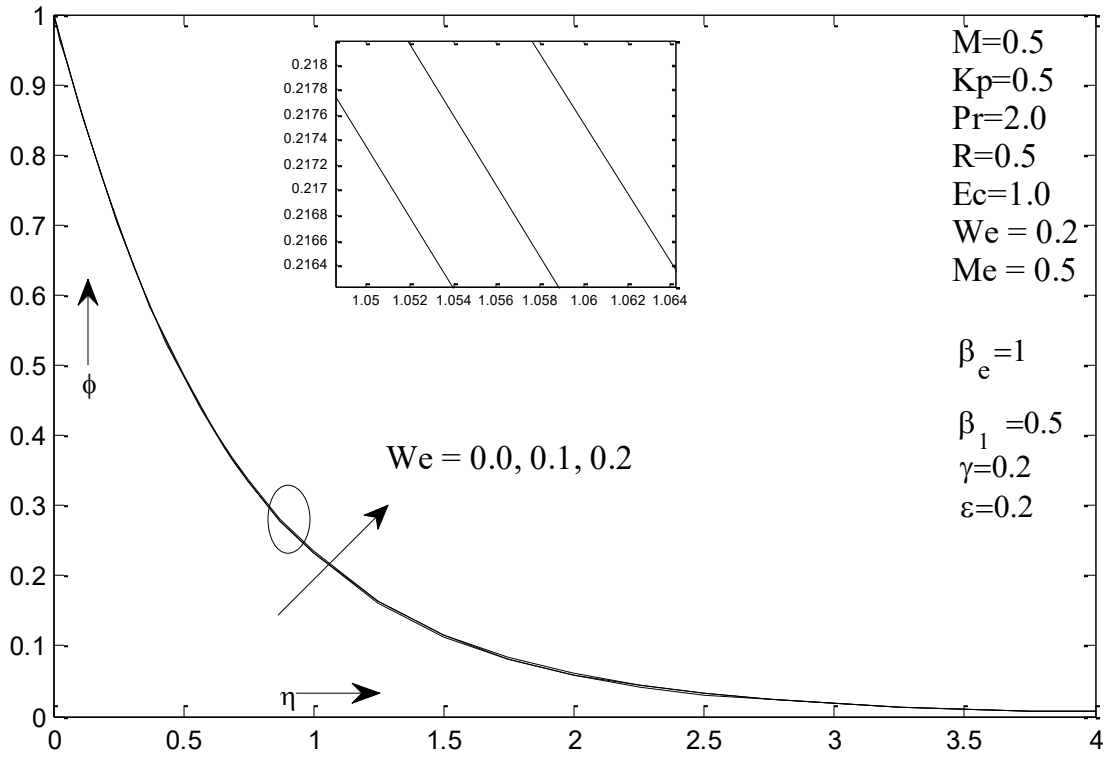

Figure 10 Influence of We on mass profile

10.48047/jocaaa.2024.33.02.55
ISSN: 1521-1398
E-ISSN: 1572-9206

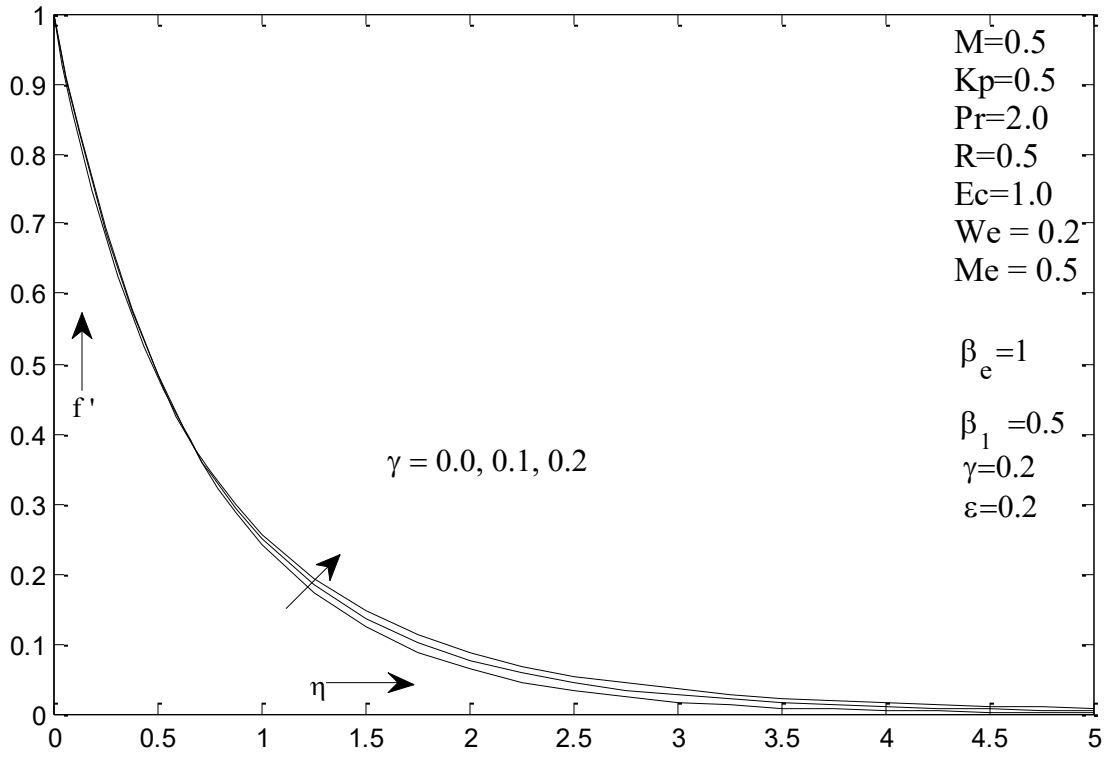

Figure 11 Influence of γ on Momentum profile

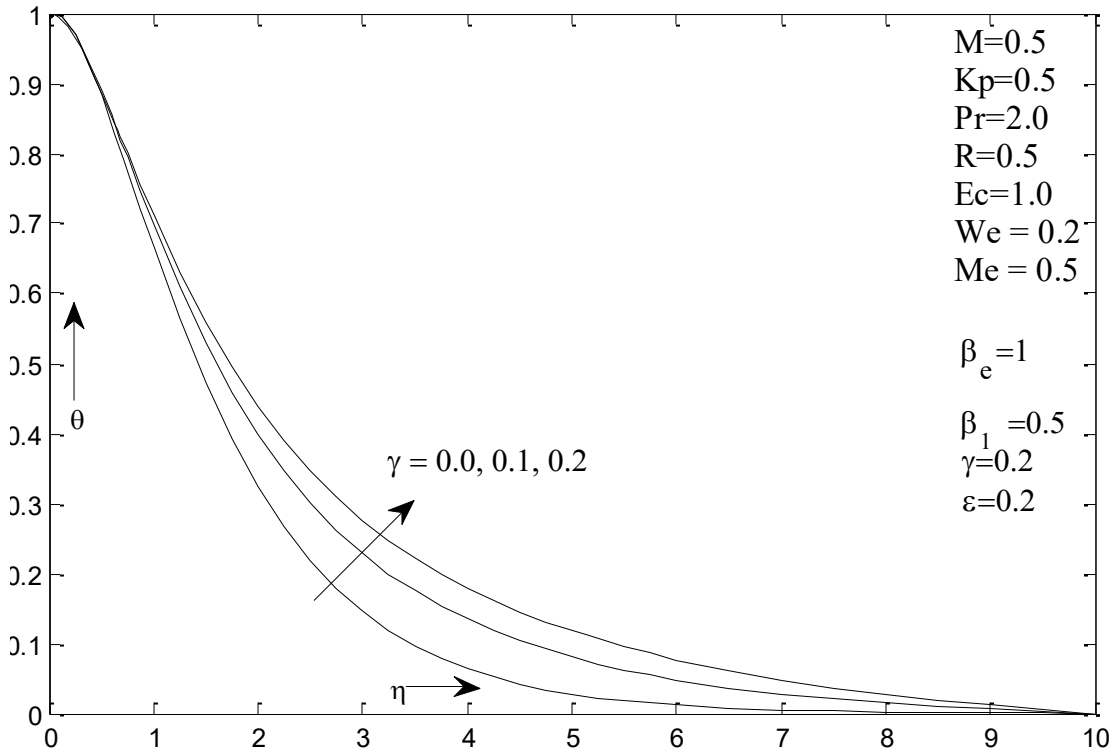

10.48047/jocaaa.2024.33.02.55
ISSN: 1521-1398
E-ISSN: 1572-9206

Figure 12 Influence of γ on Temperature profile

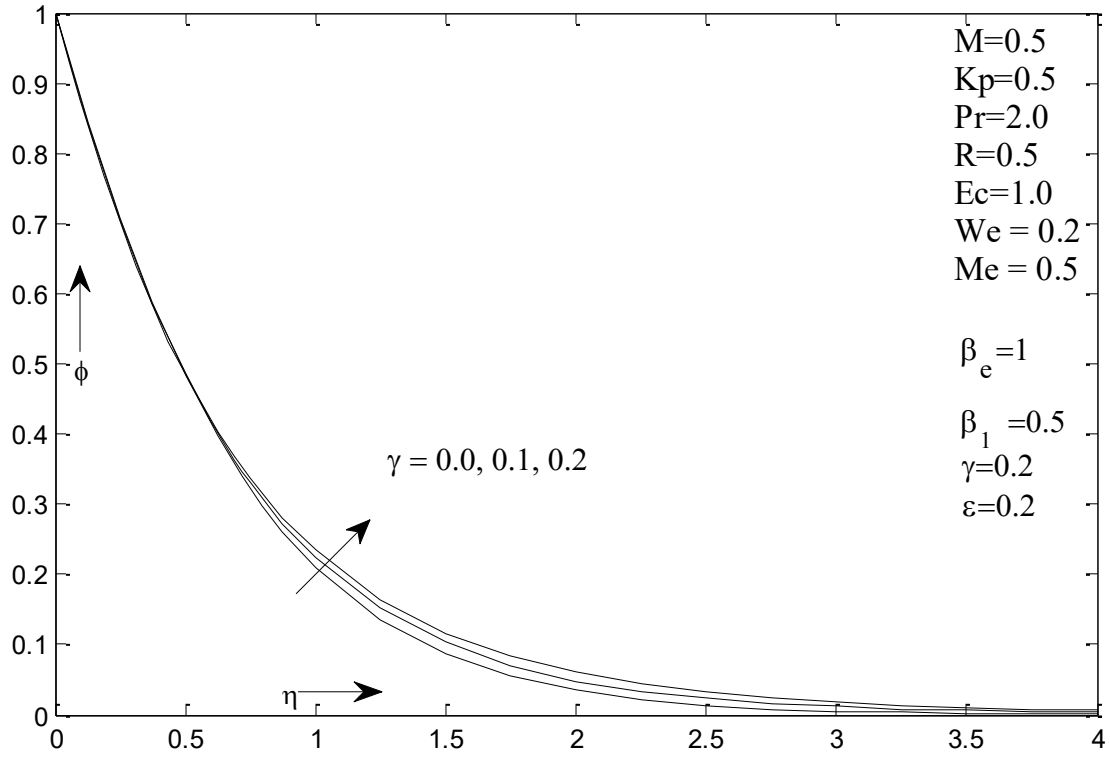

Figure 13 Influence of γ on mass profile

10.48047/jocaaa.2024.33.02.55
ISSN: 1521-1398
E-ISSN: 1572-9206

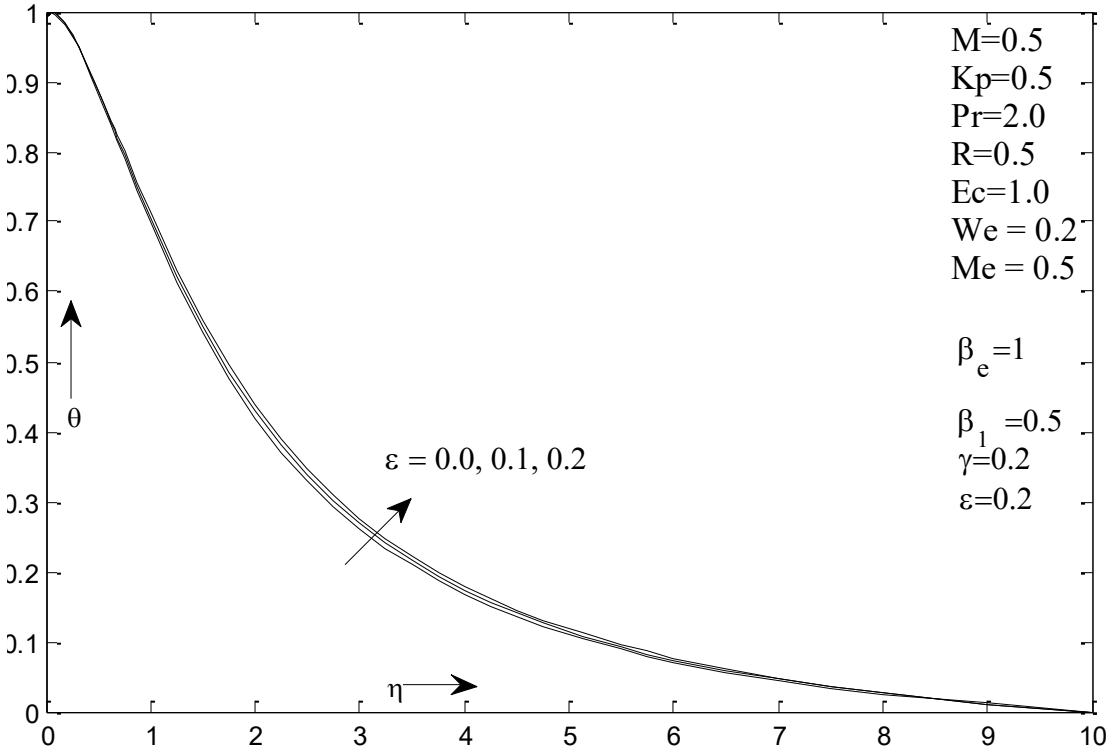

Figure 14 Influence of ε on Temperature profile

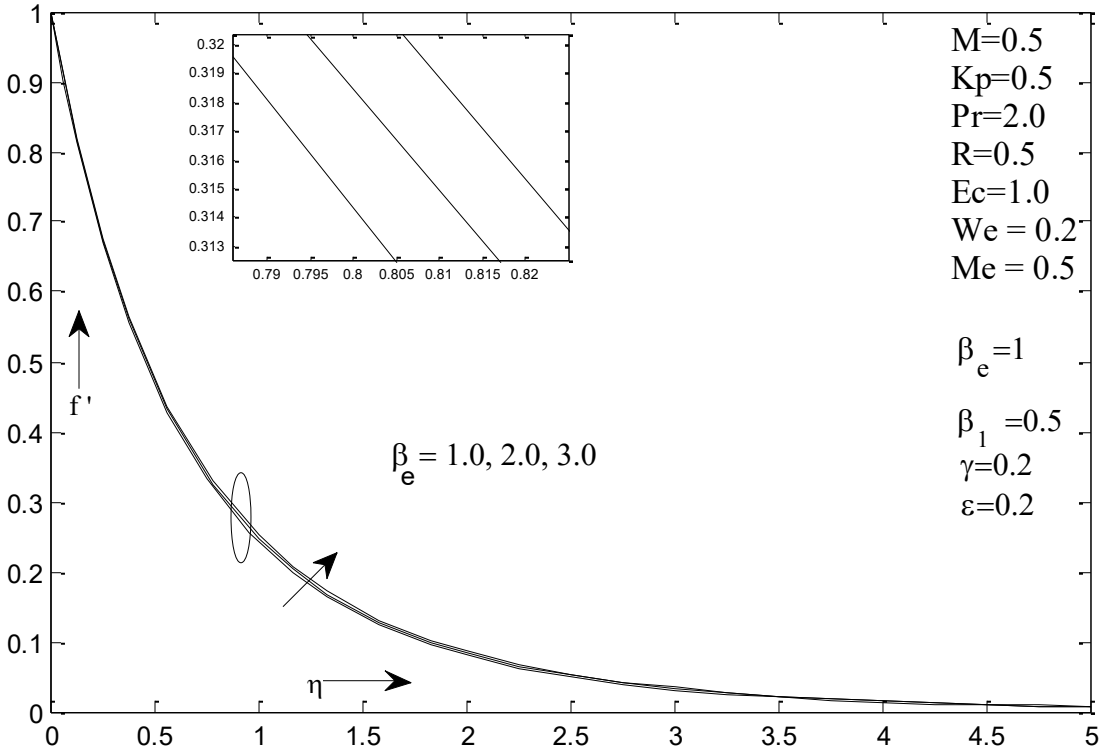

10.48047/jocaaa.2024.33.02.55
ISSN: 1521-1398
E-ISSN: 1572-9206

Figure 15 Influence of β_e on momentum profile

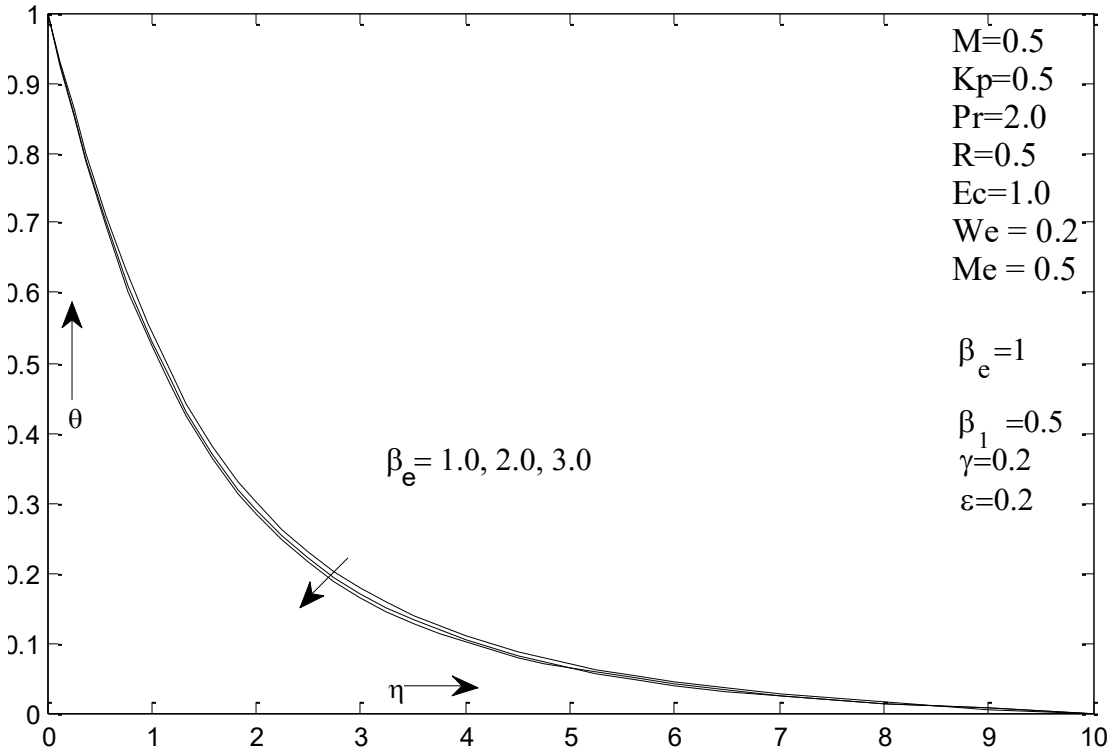

Figure 16 Influence of β_e on Temperature profile

10.48047/jocaaa.2024.33.02.55
ISSN: 1521-1398
E-ISSN: 1572-9206

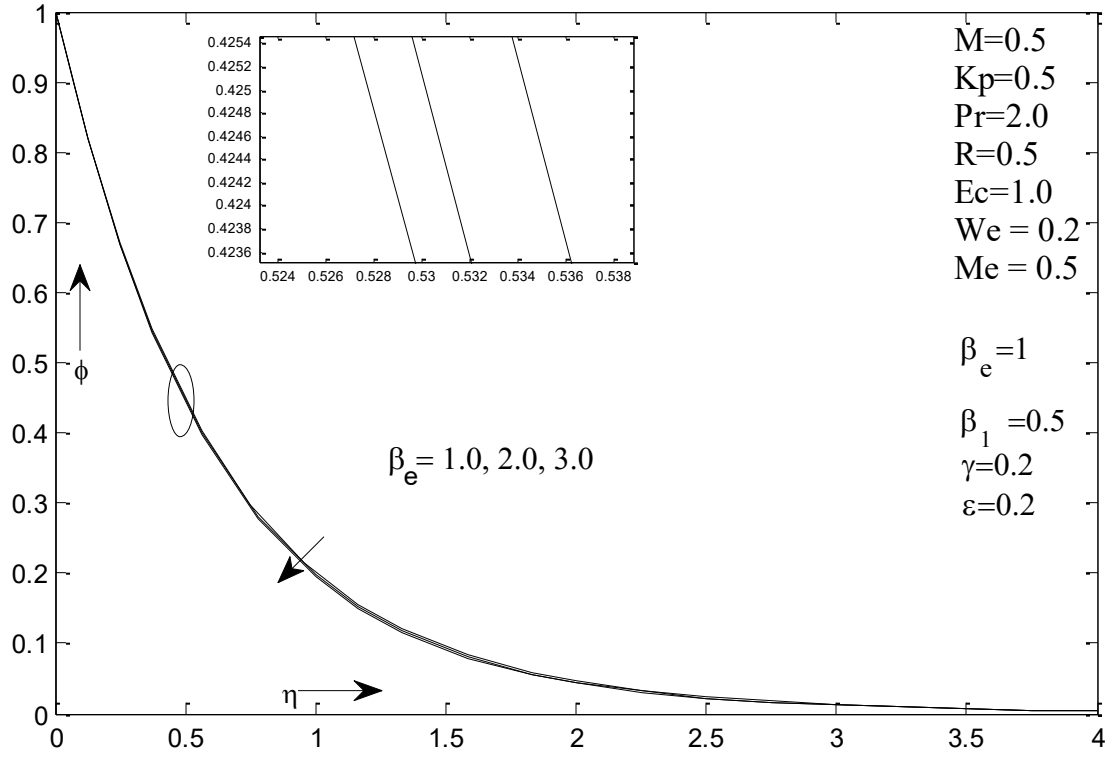

Figure 17 Influence of β_e on mass profile

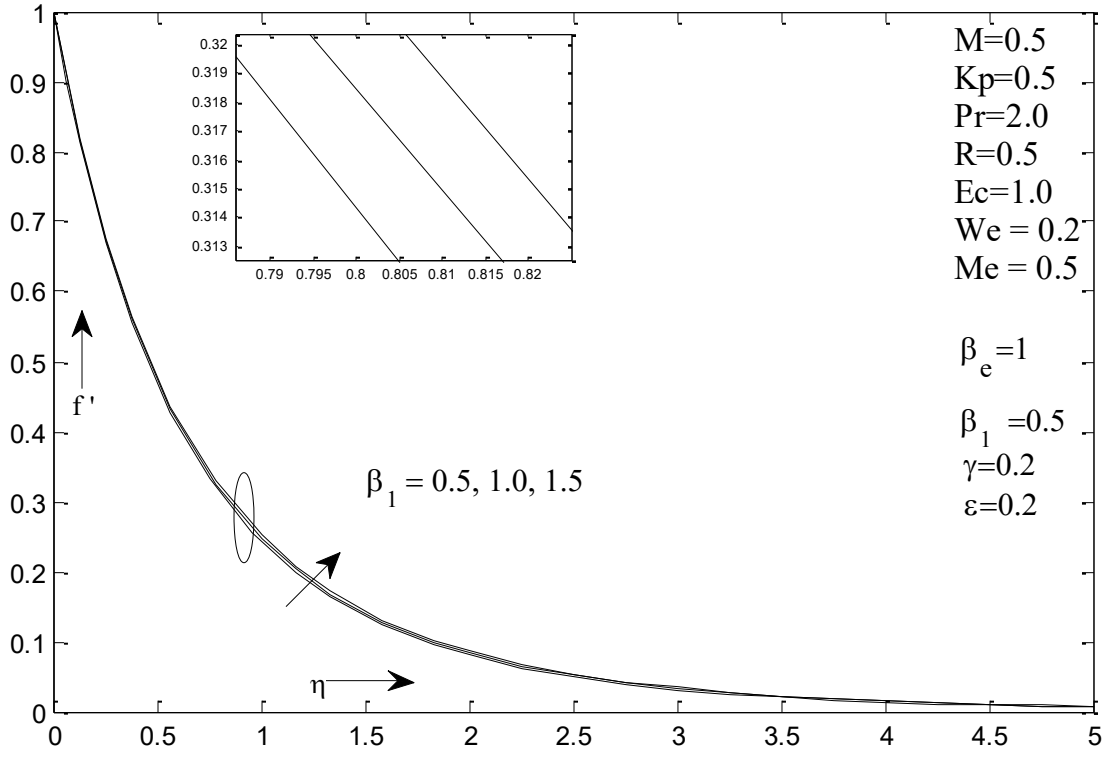

10.48047/jocaaa.2024.33.02.55
ISSN: 1521-1398
E-ISSN: 1572-9206

Figure 18 Influence of β_1 on momentum profile

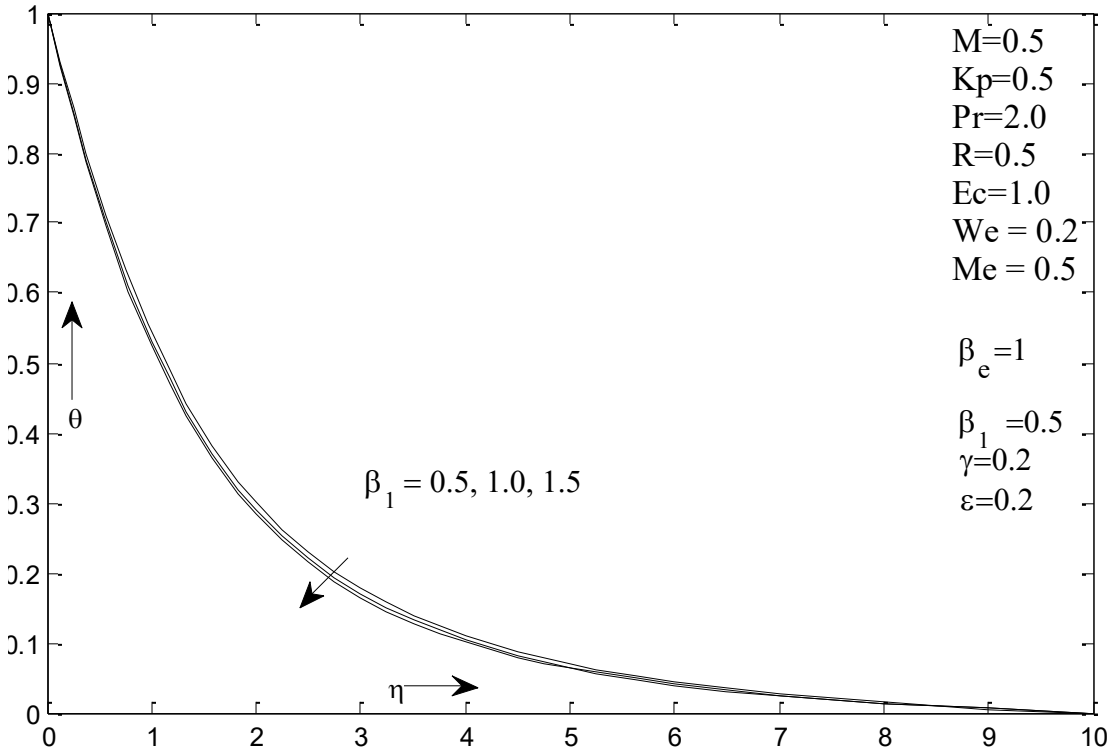

Figure 19 Influence of β_1 on Temperature profile

10.48047/jocaaa.2024.33.02.55
ISSN: 1521-1398
E-ISSN: 1572-9206

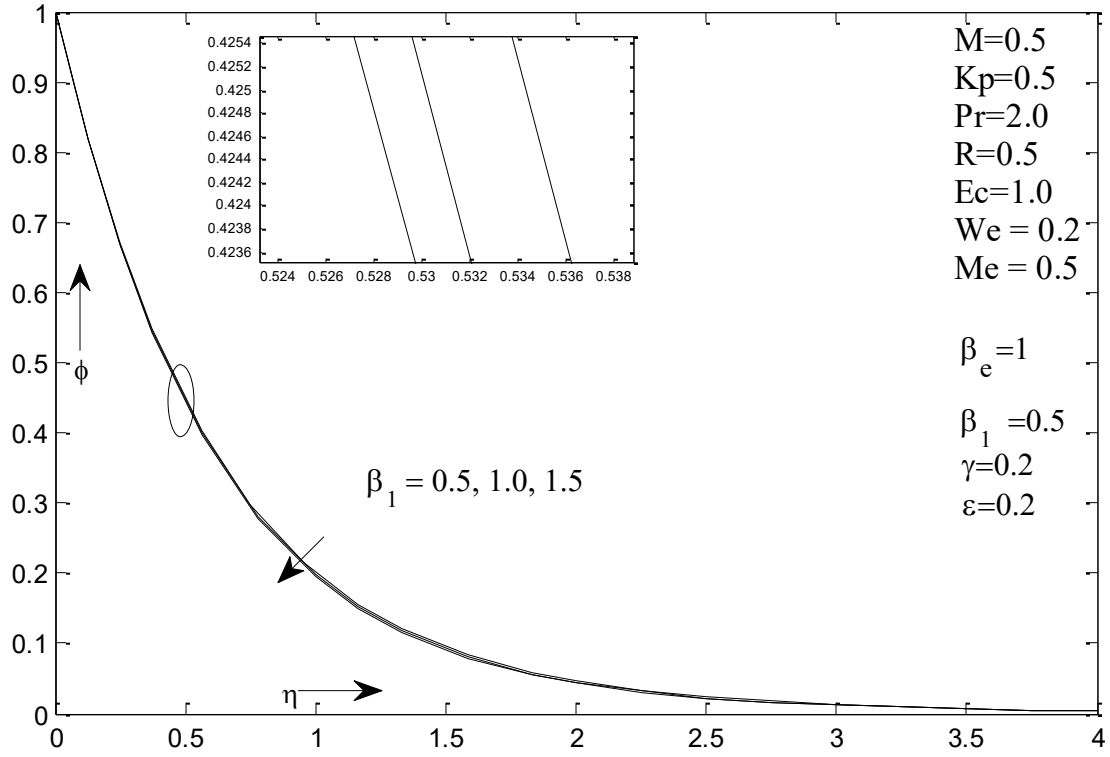

Figure 20 Influence of β_1 on mas profile

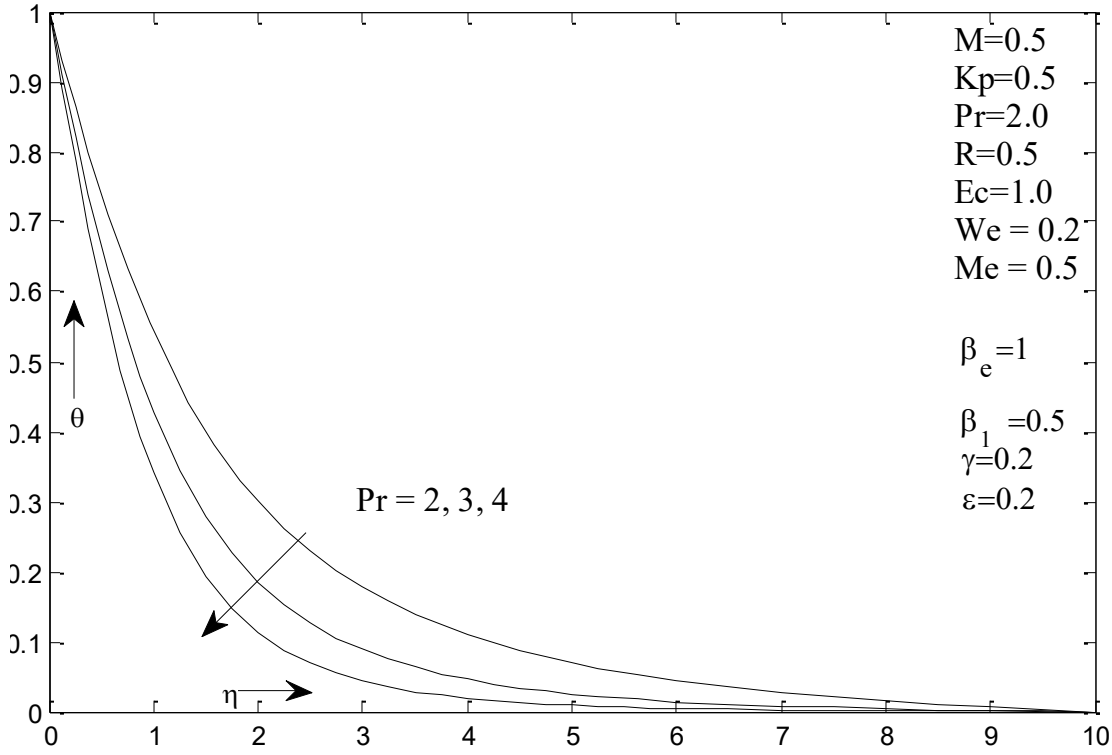

10.48047/jocaaa.2024.33.02.55
ISSN: 1521-1398
E-ISSN: 1572-9206

Figure 21 Influence of Pr on Temperature profile

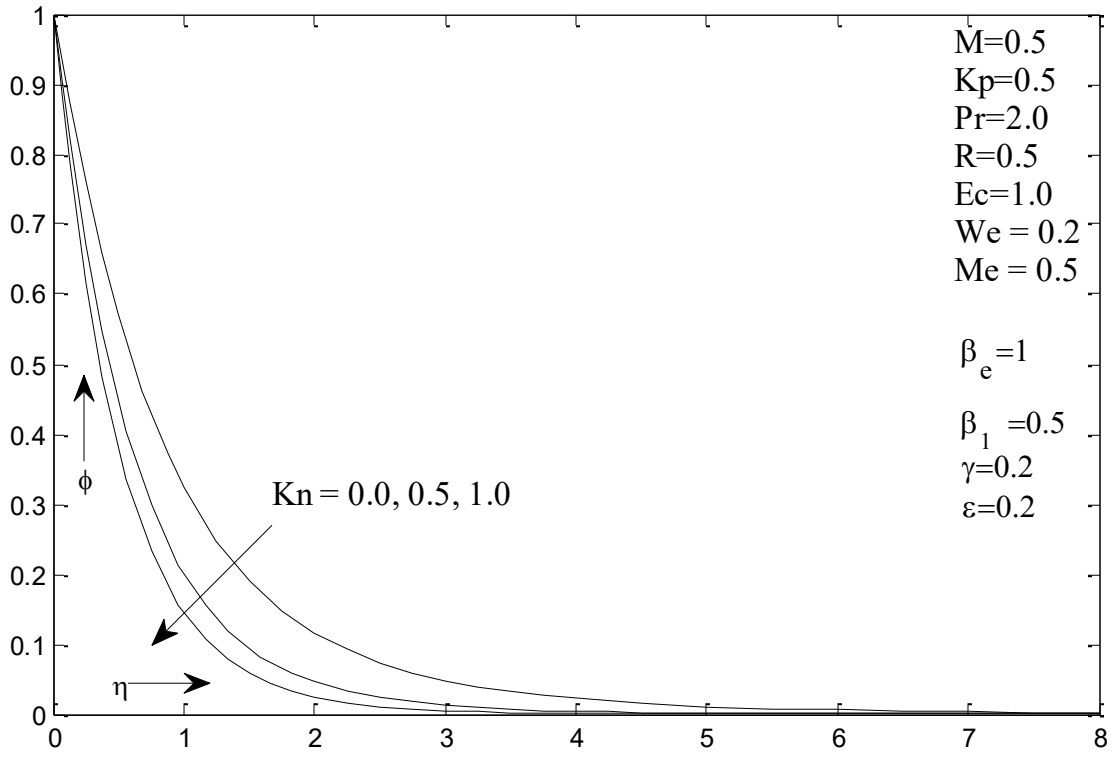

Figure 22 Influence of Kn on mass profile

10.48047/jocaaa.2024.33.02.55
ISSN: 1521-1398
E-ISSN: 1572-9206

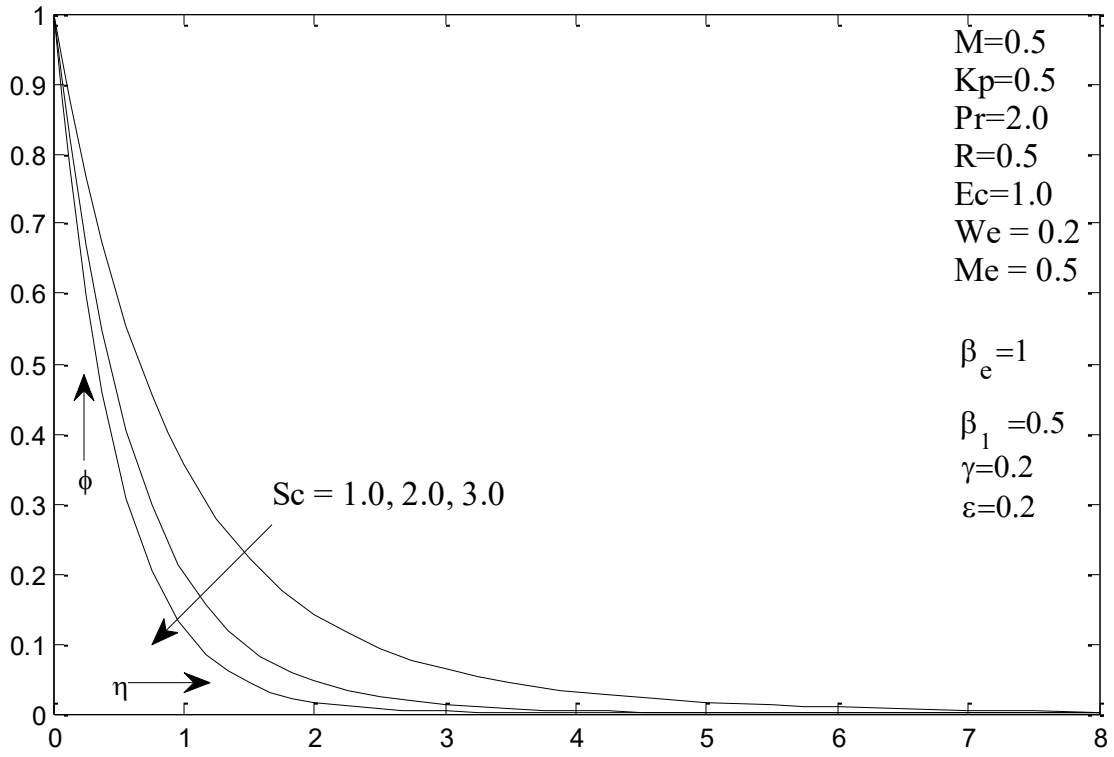

Figure 23 Influence of Sc on mass profile

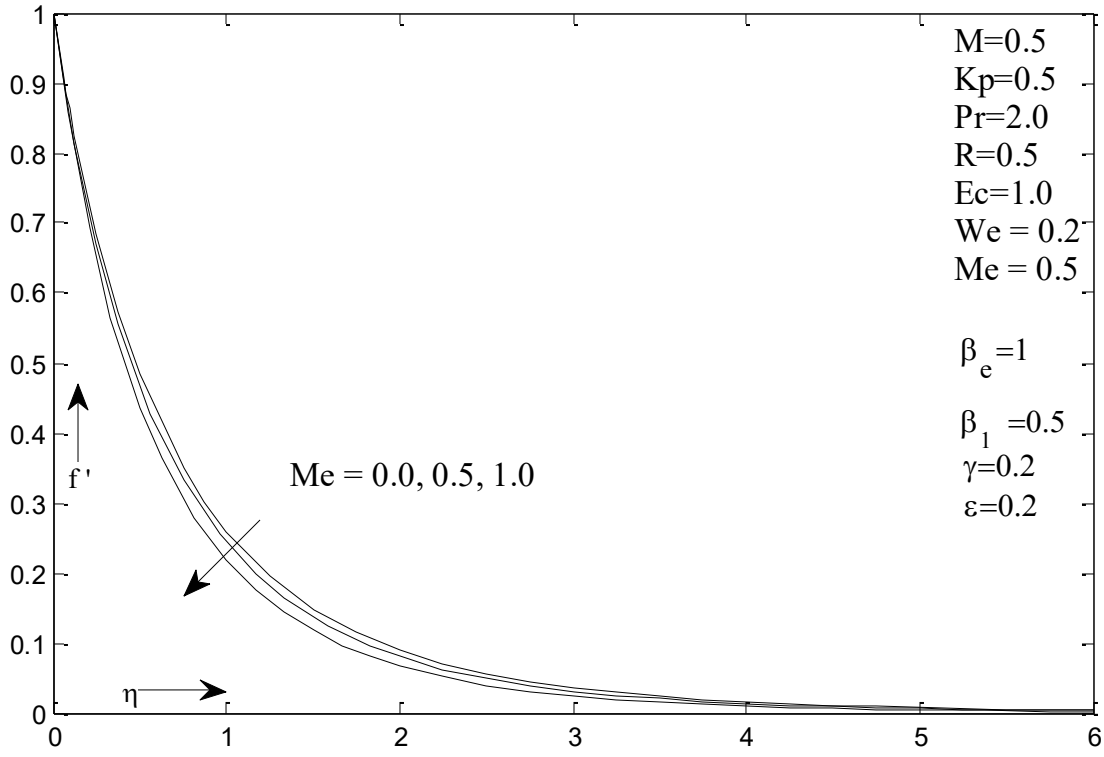

10.48047/jocaaa.2024.33.02.55
ISSN: 1521-1398
E-ISSN: 1572-9206

Figure 24 Influence of Me on momentum profile

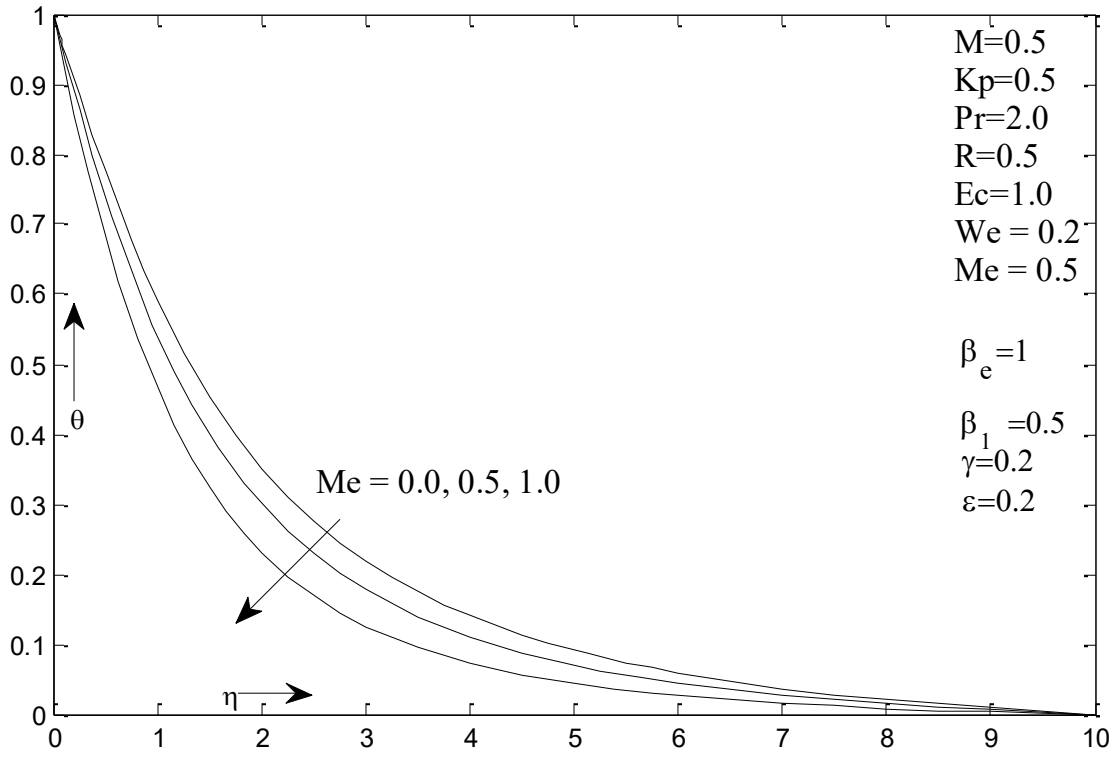

Figure 25 Influence of Me on Temperature profile

10.48047/jocaaa.2024.33.02.55
ISSN: 1521-1398
E-ISSN: 1572-9206

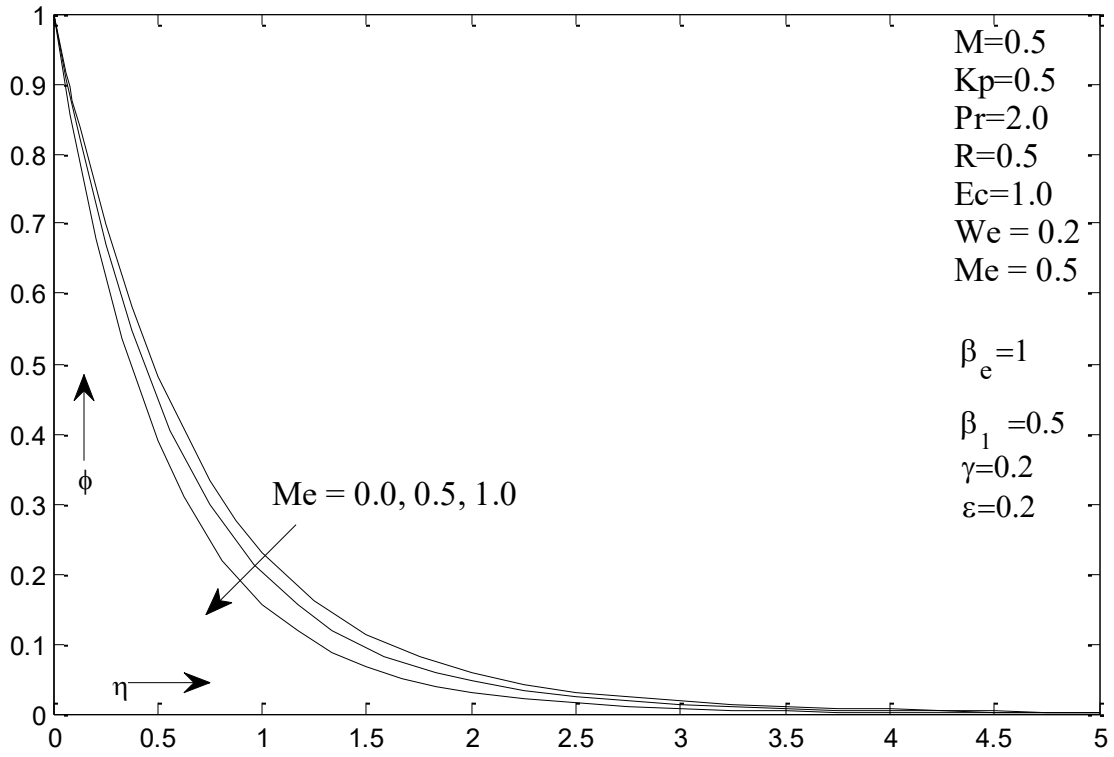

Figure 26 Influence of Me on mass profile

Table - 2

M	Kp	We	γ	ε	Pr	Kn	Sc	β_e	Me	*Cf*	Nh_x	Sh_x
0.0										-1.3380779	1.09652555	1.60215787
0.3										-1.3589899	0.38526260	1.46705525
0.5										-1.3731346	-0.06191387	1.38567459
	0.0									-1.1670757	-0.17353524	1.38944357
	0.3									-1.2851830	-0.10416540	1.38801227
	0.5									-1.3561762	-0.06954488	1.38619035
		0.0								-1.4364323	-0.11419733	1.38787605
		0.1								-1.3986410	-0.09349966	1.38716633
		0.2								-1.3561762	-0.06954488	1.38619035
			0.0							-1.2795320	-0.09634072	1.29796723
			0.1							-1.3174242	-0.09664807	1.34009864
			0.2							-1.3561762	-0.06954488	1.38619035
				0.0							-0.10834716	

10.48047/jocaaa.2024.33.02.55
ISSN: 1521-1398
E-ISSN: 1572-9206

				0.1							-0.08745015	
				0.2							-0.06954488	
					2						0.93177902	
					3						1.21830278	
					4						1.47060269	
						0.0						1.05834816
						0.5						1.56241380
						1.0						1.90771791
							1					1.06202381
							2					1.56241380
							3					1.97352460
								1.0		-1.4134591	0.93177902	1.56241380
								2.0		-1.3960281	0.99238410	1.57582276
								3.0		-1.3835683	1.02448613	1.58330914
									0.0	-1.3461272	0.77237885	1.39951749
									0.5	-1.4134591	0.93177902	1.56241380
									1.0	-1.5277710	1.21055166	1.84607449

Result and Discussion

Figs. 2–20 represent the velocity, temperature and concentration profiles. Figs. 2-4 show the influence of (M) parameter on velocity, heat and concentration profiles. As increase the (M) parameter suppress the momentum boundary layer thickness and exactly reverse effect have been observed for the heat and concentration profiles. Figs. (5-7) show the impacts of (Kp) parameter on momentum, temperature and mass profiles. Rising the (Kp) parameter suppresses the momentum profile and enhancement the thermal and concentration profiles. From figs. (8-10) it is detected that for a non-Newtonian fluids, the momentum of fluid as well as the boundary layer thickness of velocity profile decreases and temperature and concentration profile increses with the increases in (We) parameter. Figs. (11-13) show the impacts of (γ) parameter on momentum, temperature and mass profiles. Rising the (γ) parameter enhance the momentum profile, thermal profile and concentration profiles. Figs. 14 shows the influences of (ε) parameter on temperature profile. As increases the (ε) parameter, the heat profile increase. From figs. (15-20) it is detected that for a non-Newtonian fluids, the momentum of fluid as well as the boundary layer thickness of velocity profile increse and temperature and concentration profile decrease with the increases in

10.48047/jocaaa.2024.33.02.55
ISSN: 1521-1398
E-ISSN: 1572-9206

(β_e) and (β_1) parameter. Figs. 21 shows the influences of (Pr) parameter on temperature profile. As increases the (Pr) parameter, the heat profile decreases. High values of radiation parameter cause raised dominance of conduction thereby decreasing the temperature profile and Prandtl number can be used to increase the rate of cooling in conducting flows.Figs. 22-23 show the influence of Kn and Sc parameters on concentration profile. As the increase the value of Kn and Sc parameters, concentration boundary layer thickness as well as mass profile reduce. Physically, chemical reaction increases the rate of interfacial mass transfer. Chemical reaction suppresses the local concentration, thus increases its mass gradient and its flux. It is due to the fact that Sc is the ratio of velocity to mass diffusivities which means that when Sc increases, mass diffusivity decreases and there is a reduction in mass. Figs. 24-26 show the impacts of suction/injection parameter (Me) on momentum, temperature and concentration profiles. As the increase in the value of (Me) parameter, suppress the velocity, heat and concentration profiles. Table 1 shows the comparison of the present results with the existed results of Anderson et al. [27], Prasad et al. [28], Mukhopadhyay et al. [29] and Palani et al [30]. Table 2 shows the effects on various parameter on skin friction coefficient, local Nusselt number and local Sherwood number.

Conclusion:

In this work, slip-flow characteristics of a magnetohydrodynamic (MHD) Williamson fluid over a melting and stretching cylindrical surface embedded in a porous medium are examined. The effects of chemical reaction and Hall current are incorporated into the formulation. The governing partial differential equations are reduced to a system of nonlinear ordinary differential equations through appropriate similarity transformations. Numerical solutions are obtained using the shooting method combined with the classical fourth-order Runge–Kutta scheme. The main findings of the present investigation are summarized as follows:

- Higher values of the magnetic parameter M, permeability parameter Kp and Williamson parameter We diminish the momentum boundary layer and velocity field, while producing an increasing trend in the temperature and concentration distributions.
- Larger values of β_e and β_1 lead to an expansion of the momentum boundary layer, whereas the thermal and concentration boundary layers decrease correspondingly.
- Increases the value of (γ) rises momentum boundary layer thickness, heat flux as well as temperature profile and concentration profile whereas opposite effects show to increase the value of (Me) on momentum, temperature and concentration profiles.
- It is observed that the skin-friction and local Nusselt number increases whereas local Sherwood number decreases as the value of (We) and (Kp) increases.

10.48047/jocaaa.2024.33.02.55
ISSN: 1521-1398
E-ISSN: 1572-9206

- Skin-friction, local Nusselt number and local Sherwood number decreases as the value of (M) increases.
- Skin-friction, local Nusselt number and local Sherwood number increases as the value of (β_e) increases.
- It is observed that the skin-friction decreases whereas local Nusselt number and local Sherwood number increases as the value of (Me) increases.
- Local Nusselt number increases along with the increasing values of the (Pr) and (ε).
- Local Sherwood number increases along with the increasing values of the (Sc) and (Kn).

Reference

[1]. Alam N, Khan H, Khan A (2014) boundary layer flows of non-Newtonian Williamson fluid, Nonlinear Eng. 3(2): 107–115.
[2]. Williamson RV (1929) The flow of pseudo plastic materials, Ind. Eng. Chem. 21: 1108–1111.
[3]. Dapra I, Scarpi G (2007) Perturbation solution for pulsatile flow of a non-Newtonian Williamson fluid in a rock fracture, Int. J. Rock Mech. Min. Sci. 44: 271–278.
[4]. Gorla RSR, Gireesha BJ (2016) Dual solutions for stagnation-point flow and convective heat transfer of a Williamson nanofluid past a stretching/shrinking sheet, Heat Mass Transfer 52: 1153–1162.
[5]. Khan NA, Khan S, Riaz F (2014) Boundary layer flow of Williamson fluid with chemically reactive species using scaling transformation and homotopy analysis method, Math Sci Lett 3(3):199-205.
[6]. Monica M, Sucharitha J, Kumar CK (2016) Stagnation point flow of a Williamson fluid over a nonlinearly stretching sheet with thermal radiation. American Chemical Science Journal 13(4): 1-8.
[7]. Gorla RSR, Prasannakumara BC, Gireesha BJ, Krishnamurthy MR (2016) Effects of chemical reaction and nonlinear thermal radiation on Williamson nanofluid slip flow over a stretching sheet embedded in a porous medium, J. Aerosp. Eng. 29(5): 04016019.
[8]. Nadeem S, Hussain ST, Lee C (2013) Flow of a Williamson fluid over a stretching sheet, Braz. J. Chem. Eng. 30 (3): 619–625.
[9]. Nadeem S, Hussain ST (2014) Heat transfer analysis of Williamson fluid over exponentially stretching surface, Appl. Math. Mech. Engl. Ed. 35 (4): 489–502.
[10]. Nadeem S, Akbar NS (2010) Numerical solutions of peristaltic flow of Williamson fluid with radially varying MHD in an endoscope, Internat. J. Numer. Methods Fluids 66: 212–220.
[11]. Nadeem S, Hussain ST (2014) Flow and heat transfer analysis of Williamson nanofluid, Appl. Nanosci. 4: 1005–1012.
[12]. Humane PP, Patil VS, Patil AB, Shamshuddin MD, Rajput GR (2022) Dynamics of multiple slip boundaries effect on MHD Casson-Williamson double-diffusive nanofluid flow past an inclined magnetic stretching sheet. Proceedings of the Institution of Mechanical Engineers, Part E: Journal of Process Mechanical Engineering 236(5):1906-1926.

10.48047/jocaaa.2024.33.02.55
ISSN: 1521-1398
E-ISSN: 1572-9206

[13]. Humane PP, Patil VS, Patil AB (2021) Chemical reaction and thermal radiation effects on magnetohydrodynamics flow of Casson–Williamson nanofluid over a porous stretching surface. Proceedings of the Institution of Mechanical Engineers, Part E: Journal of Process Mechanical Engineering 235(6):2008-2018.

[14]. Roy NC, Saha G, Saha SC (2023) Williamson Fluid Flow Having Microorganisms Over a Permeable Shrinking Sheet. Science & Technology Asia, *28*(3):1–17.

[15]. Kumari M, Jain S (2019). Variable fluid property for MHD viscous fluid containing gyrotactic microorganisms flow over a permeable stretching sheet. International Journal of Heat and Technology, 37(3):766-778. https://doi.org/10.18280/ijht.370313.

[16]. Nadeem S, Hussain ST (2016) Analysis of MHD Williamson nano fluid flow over a heated surface, J. Appl. Fluid Mech. 9: 729–739.

[17]. Shalini Jain, Manjeet kumari, Amit Parmar (2018) Unsteady MHD chemically reacting mixed convection nano-fluids flow past an inclined pours stretching sheet with slip effect and variable thermal radiation and heat source, Materials Today: Proceedings, 5(2):6297-6312.

[18]. Malik MY, Uddin TS (2015) Numerical solution of MHD stagnation point flow of Williamson fluid model over a stretching cylinder. International Journal of Nonlinear Sciences and Numerical Simulation 16:161–164.

[19]. Darji RM, Timol MG (2014) On invariance analysis of MHD boundary layer equations for non-Newtonian Williamson fluids. Int J Adv Appl Math and Mech 1(4):10 – 19

[20]. Narayana KL, Gangadhar K, Subhakar MJ (2015) Effect of viscous dissipation on heat transfer of magneto-Williamson nano fluid. IOSR J of Math (IOSR-JM) 11: 4

[21]. Roberts L (1958) On the melting of a semi-infinite body of ice placed in a hot stream of air," Journal of Fluid Mechanics 4:505–528.

[22]. Tien C, Yen Y (1965) The effect of melting on forced convection heat transfer," Journal of Applied Meteorology 4(4);523–527.

[23]. Epstein M, DH Cho (1976) Melting heat transfer in steady laminar flow over a flat plate, Journal of Heat Transfer, 98(3):531–533.

[24]. Gorla RS, Chamkha AJ, Al-Meshaiei E (2012) Melting heat transfer in a nanofluid boundary layer on a stretching circular cylinder," Journal of Naval Architecture and Marine Engineering9(1):1–10.

[25]. Kumari M., Jain S., (2019) MHD Convective Boundary Layer Falkner-Skan Flow for Powell-Eyring Fluid Over a Permeable Moving Wedge with Heat Source, 8: 938-946.

[26]. Gorla RSR, Krishnamurthya MR, Prasannakumara BC, Gireesha BJ (2016) Effect of chemical reaction on MHD boundary layer flow and melting heat transfer of Williamson nanofluid in porous medium, Engineering Science and Technology, an International Journal 19: 53–61.

[27]. Andersson, H. I., O. R. Hansen, and B. Holmedal (1994) Diffusion of a chemically reactive species from a stretching sheet. Int J Heat Mass Transfer, 37, 659–64.

[28]. Prasad, KV, Sujatha A, Vajravelu K, and Pop I (2012) MHD flow and heat transfer of a UCM fluid over a stretching surface with variable thermos-physical properties. Meccanica 47:1425–39.

[29]. Mukhopadhyay S, Golam AM, Wazed AP (2013) Effects of transpiration on unsteady MHD flow of an UCM fluid passing through a stretching surface in the presence of a first order chemical reaction. Chin Phys B 22:124701.

10.48047/jocaaa.2024.33.02.55
ISSN: 1521-1398
E-ISSN: 1572-9206

[30]. Palani S, Kumar BR, Kameswaran PK (2016) Unsteady MHD flow of an UCM fluid over a stretching surface with higher order chemical reaction. Ain Shams Engineering Journal 7: 399–408.